

ULTRASONIC REFLECTION FROM ROUGH SURFACES IN WATER

James H. Rose and David K. Hsu

Ames Laboratory, USDOE
Iowa State University
Ames, IA 50011

INTRODUCTION

The use of ultrasound for immersion mode quantitative nondestructive evaluation depends on our ability to model the interaction of the incident beam with the water-solid interface. The effects of surface roughness on the inspection process may be crucial. For example, ultrasonic images of interior flaws will be degraded due to the random fluctuations in the wave front of the incident field [1,2]. Similarly, surface roughness also affects the characterization of porosity in solids from the ultrasonic attenuation [3] since the attenuation is commonly determined by comparing the reflection from the backsurface with that from the front surface of the part.

Our study parallels a recent paper by Adler et al. [4] who studied the reflection as a function of frequency from a rough crack in the interior of a solid. They asserted that the low frequency part of the signal determined the root-mean-square (r.m.s.) surface roughness, while the high frequency part of the signal could be associated with a correlation length parallel to the surface. These assertions, taken by analogy, form the basic hypotheses of our experiment. We report a preliminary experimental study of the ultrasonic reflection from the randomly rough (but otherwise flat) front surfaces of model samples immersed in water. Our work differs from Ref. 4 in a further way. Namely, the r.m.s. roughness of our samples varied by a factor of roughly 8, while they restricted their study to a single sample. Finally, our work concerns itself with the frequency dependence of the reflected signal and the size of the transducer. Consequently, it differs substantially from recent oceanographic studies of the sea bed.

The organization of the paper is as follows. First, we report experimental measurements in the pulse-echo mode using a conventional phase-sensitive immersion transducer (see Fig. (1)). Next, we describe the general features of the resulting signals. These features are then analyzed on a physical basis with special attention at low and high frequencies. Finally, we compare the results with our hypothesis.

Basically, we find that the r.m.s. surface roughness correlates directly with the long wavelength part of the signal. A single comparison indicated no strong effects due to the transducer size. The high frequency

portion of the signal correlates rather weakly with size of the scatterers parallel to the surface. These measurements were found to depend on the ratio of a to R , where a indicates the size of a typical scatterer and R is the radius of the transducer.

Experiment

The experimental measurement configuration is shown in Fig. 1. A broadband ultrasonic pulse is launched from an immersion transducer whose axis is oriented normally with respect to the part's surface. The sound pulse travels a distance z_0 and is reflected at the rough surface. Then it is detected by the same transducer operating in the receiving mode. The signal is digitized and the amplitude of its frequency domain Fourier transform, $|A(\omega)|$, is then obtained. The signal $|A(\omega)|$ is usually quite "noisy" due to the random interference caused by the different heights of various parts of the rough surface. To extract average properties of the rough surface it is useful to spatially average the signal. This is accomplished by repeating the measurement while moving the transducer by a small distance parallel to the surface each time and then taking the average. The result is

$$\langle |A(f)| \rangle \equiv \frac{1}{N} \sum_{j=1}^N |A_j(f)|. \quad (1)$$

Here $|A_j(f)|$ denotes the signal obtained with the j th measurement while f denotes the frequency. Finally, to obtain the signal due to the surface roughness $\langle |A(f)| \rangle$ is normalized by the reflection $|A_0(f)|$ from a smooth surface. We will display the logarithmic difference of these two spectra

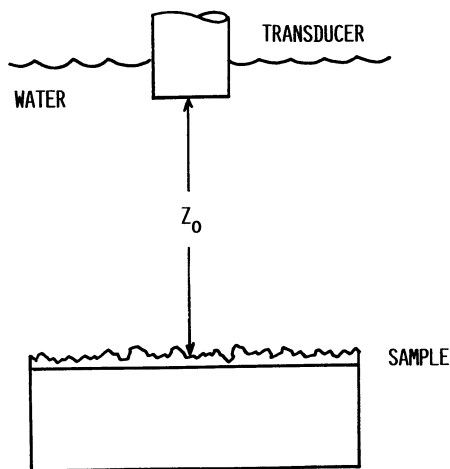


Fig. 1. Shows the geometry of the experiment.

$$S(f) \equiv -\ln \left[\frac{\langle |A(f)| \rangle}{|A_0(f)|} \right]. \quad (2)$$

This method has the advantage of eliminating the effects of diffraction to a large extent since the path length in the two measurements are kept the same.

Waterproof sandpapers were used as convenient models of randomly rough surfaces where the scattering centers (i.e., the sand grain) were approximately the same size. The sandpapers were glued onto a brass block and the transducer was placed 3.7cm from the surface. The transducer diameter for all but one set of measurements was 1/4" (there were two of these transducers with nominal center frequencies of 10 and 20MHz). Also, a 1/2" diameter transducer with a nominal center frequency of 10MHz was used. In the averaging process the number of samples is typically 10 to 20.

The measured signals will now be described. Figures 2(a)-2(e) shows the ultrasonic signal $S(f)$ for a variety of grit sizes. The conversion from grit size to grain diameter is given in Table I. The signal increases rapidly and monotonically at low frequencies. At high frequencies $S(f)$ appears to become roughly constant. We note that the low frequency portion of $S(f)$ varies strongly with grit size and hence surface roughness. For example, the strength of the reflection at 4MHz varied roughly by a factor of five as the average grit diameter varied from 78 μ m to 406 μ m. On the other hand, the high frequency plateau varied rather weakly (by a factor of 1.2) for the same grit size range.

Table I. Conversion from grit size to the nominal diameter of the sand grains.

Grit Number	Grain Diameter (μ m)
60	400
80	266
100	173
120	142
150	122
180	70-86

The sandpaper consists of grains of sand glued to a paper backing. Figure 3A shows the surface of the 120 grit sample. A cutaway section of the same sample is shown in Fig. 3B; one can see the paper (bottom), the glue and the sand grains which extend from the upper surface. Photographs like Fig. 3B were used to estimate the r.m.s. roughness. For the 120 grit sample the r.m.s. roughness was found to be 40 μ m, or 0.28 of the nominal grit diameter.

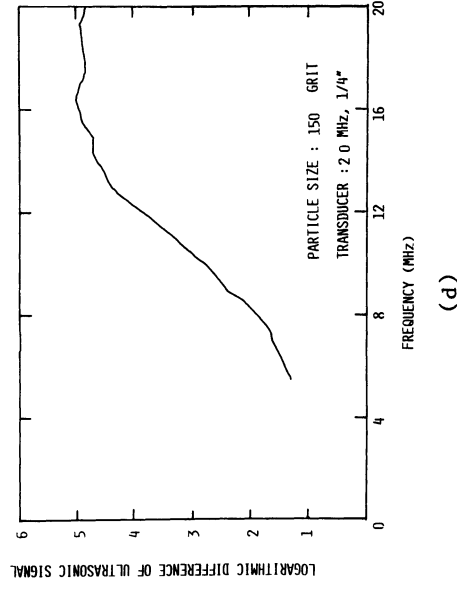
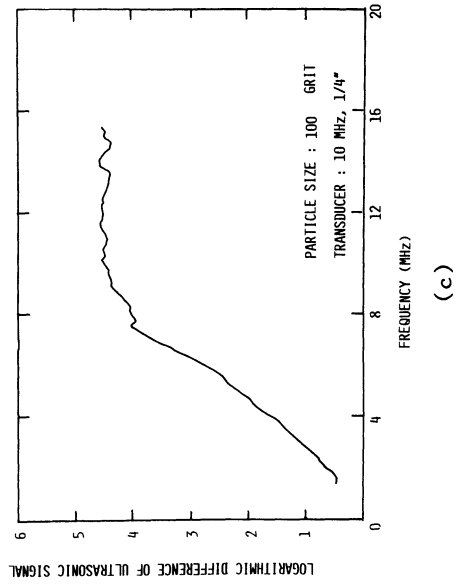
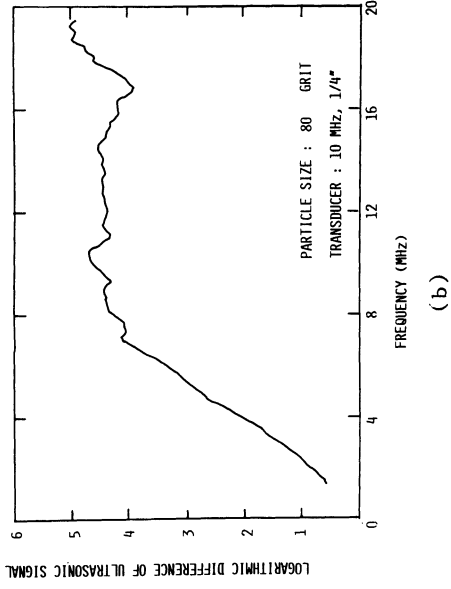
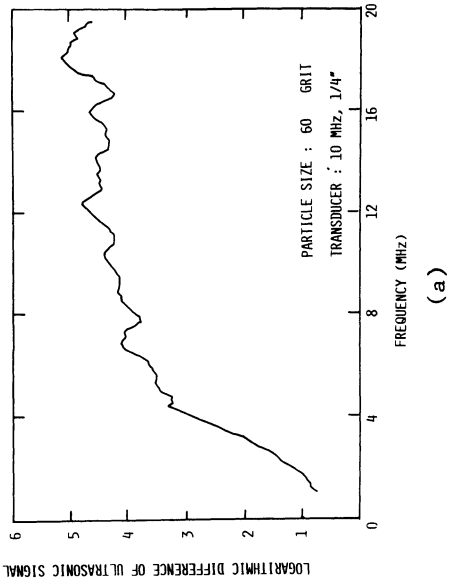


Fig. 2. Shows the signal $S(f)$ for a variety of grit sizes.

Physical Nature of the Signal

The transducer measures the total displacement of its surface induced by the pressure field in the water. Consider an impulse launched from the transducer, reflected by a rough surface and then detected by the same transducer. In the absence of roughness and diffraction the reflected displacement amplitude would be a single impulse at time $t=2z_0/v_w$ where

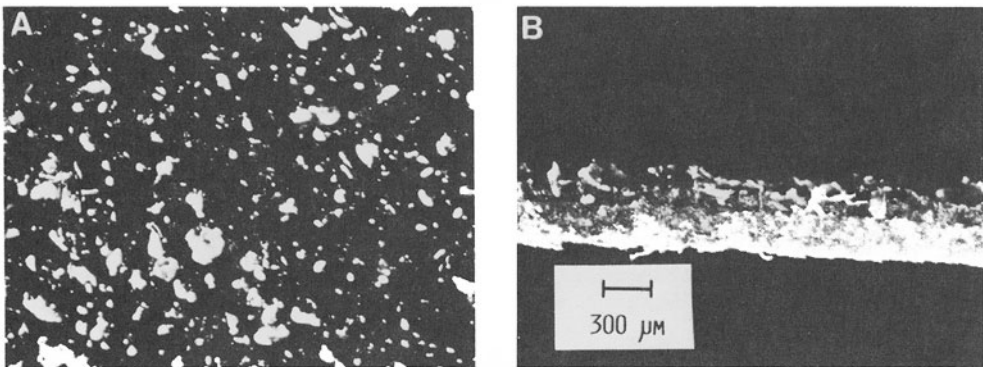


Fig. 3. (A) Shows surface of 120 grit sandpaper, (B) shows cutaway section of 120 grit sandpaper. The sand grains are shown protruding from upper surface.

z_0 is the distance from the transducer's face to the sample's surface and v_w is the velocity of sound in water. The effect of surface roughness is to cause certain portions of the wavefront to be reflected at different times. The consequent interference between the various portions of the wavefront reduces the amplitude of the coherent part of the signal.

The frequency domain interpretation of the signal allows further development. First, we write the signal for a given experiment as

$$A(\omega) = \langle A(\omega) \rangle + \delta A(\omega) \quad (3)$$

Here $\langle A(\omega) \rangle$ denotes the coherent part of the signal and $\delta A(\omega)$ denotes the fluctuating part of the signal; that is, $\langle A(\omega) \rangle$ is determined by averaging over an ensemble of samples and is given by the mean

$$\langle A(\omega) \rangle = \frac{1}{N} \sum_{j=1}^{\infty} A_j(\omega). \quad (4)$$

At low frequencies the randomness introduces only small changes in the phase and consequently minor fluctuations $\delta A(\omega)$, which in turn reduce the coherent signal by a small amount. Consequently, the coherent part of the reflected wave is much larger than the incoherent part. It is known that the coherent part of the signal due to a reflected plane wave (i.e., for an infinite transducer) is given by

$$S_{\text{coh}}(f) = -2 \frac{\overline{\Delta z}^2}{\Delta z^2} f^2. \quad (5)$$

Here $\overline{\Delta z}$ is the r.m.s. roughness. As a result, the long wavelength part of the signal determines the r.m.s. roughness in the plane wave case.

As the frequency increases, the phase difference between different parts of the wavefront grows. We can model this process as follows. The transducer illuminates a circular region of the sample. Within this region there are N independent scattering sites. These are the various grains plus the regions of glue between the grains which are exposed to the surface. For the sake of simplicity we assume that each scatterer reflects its portion of the beam specularly back along the axis of the transducer. The phase from each scatterer is then given by $\exp(2ikz_j)$ where k is the wavevector of sound in water and z_j denotes the distance from the transducer face to a given scattering site. The transducer's output is proportional to the average displacement at its surface. That is, at high frequency,

$$A(k) = \frac{T(k)}{\pi R^2} \sum_{j=1}^N \alpha_j e^{2ikz_j}. \quad (6)$$

Here $T(k)$ is a system transfer function, α_j is the area of the j th scatterer and πR^2 is the area of the transducer (which has radius R).

At sufficiently high frequencies ($k\overline{\Delta z} \gg 1$) the phase varies randomly from scatterer to scatterer. Consequently, the sum in Eq. (6) reduces to a sum of random numbers with weights α_j . The result for an ensemble average is

$$\langle |A(k)| \rangle = \frac{T(k) N \bar{\alpha}}{\pi R^2}. \quad (7)$$

where $\bar{\alpha}$ is the average area of a scatterer. Using $N = \pi R^2 / \bar{\alpha}$, and the result of Eq. (6) for a smooth scatterer $|A_0(\omega)| = |T(k)|$, one obtains for $k\overline{\Delta z} \gg 1$

$$S(f) = \ln \frac{\langle |A(k)| \rangle}{|A_0(k)|} = -\frac{1}{2} \ln \left(\frac{a}{R} \right). \quad (8)$$

Here a is defined as the radius of the average scatterer via $\pi a^2 = \bar{a}$. That is, the value of $S(f)$ is expected to be constant in the plateau region and to depend logarithmically on the transducer radius and scatterer size. Equation (8) is consistent with the nearly constant value of $S(f)$ observed in the experiment. We note that the high frequency variation of $S(f)$ will depend on the morphology and orientation of the scatterers. Our derivation basically assumes that the scatterers are flat facets with their faces parallel to the surface of the part. Other approximations for the morphology of the roughness may result in $S(f)$ increasing slowly (e.g., $\ln(f)$) at high frequencies.

RESULTS

Equation (5) was used to predict the r.m.s. roughness from the data given in Fig. 2. The result is shown in Fig. 4. As can be seen, there is a good correlation between $\bar{\Delta z}$ computed ultrasonically and the grit size. Roughly we find the following fit

$$\bar{\Delta z} = 1/4 \lambda. \quad (9)$$

where λ is the grit diameter. The value of the coefficient in Eq. (9) is in excellent agreement with the value of 0.28 which was obtained by optical measurement for the 120 grit sample.

The height of the plateau is plotted in Fig. 5 as a function of grit size. As can be seen, these values are relatively insensitive to the grit size. In particular, for larger grit sizes, the values are nearly constant. Consequently, one may expect this to be an insensitive way of inferring the size of scatterers parallel to the surface (i.e., the correlation length).

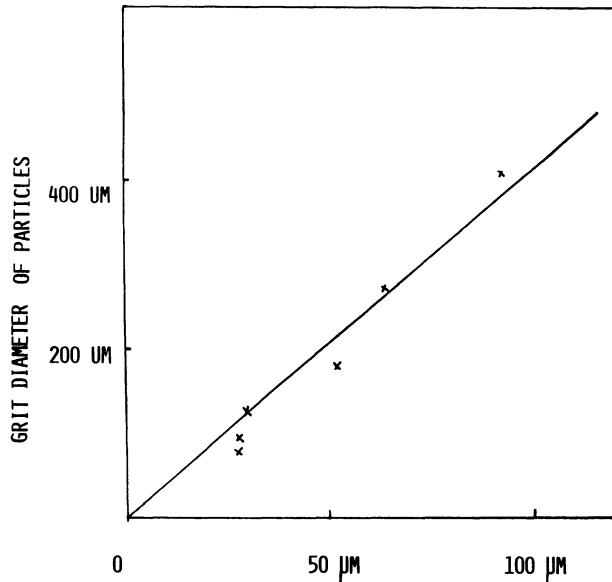


Fig. 4. The x's show the ultrasonic estimate of the r.m.s. roughness compared to the diameter of the sand grains. The straight line is the fit.

Finally, we attempted to check the functional dependence of Eq. (8) by varying the transducer radius by a factor of two. Fig. 6 shows the results of the comparison. The difference in the plateau value here is .70 which is in good agreement with $\ln 2$ (as predicted by Eq. (8)).

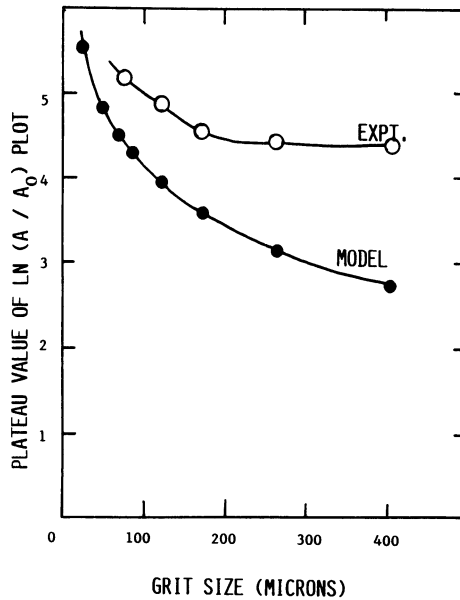


Fig. 5. Shows the value of the plateau region as a function of grit size. The model results are from Eq. (8).

SUMMARY

We have conducted a preliminary study of the effects of transducer size on the reflection from model rough surfaces. The low frequency portion of the signal (i.e., the coherent signal) was consistent with no transducer size effect. However, the high frequency portion of the signal (i.e., the incoherent signal) depended explicitly on the transducer radius. This dependence was consistent with $S \sim -1/2 \ln(a/R)$.

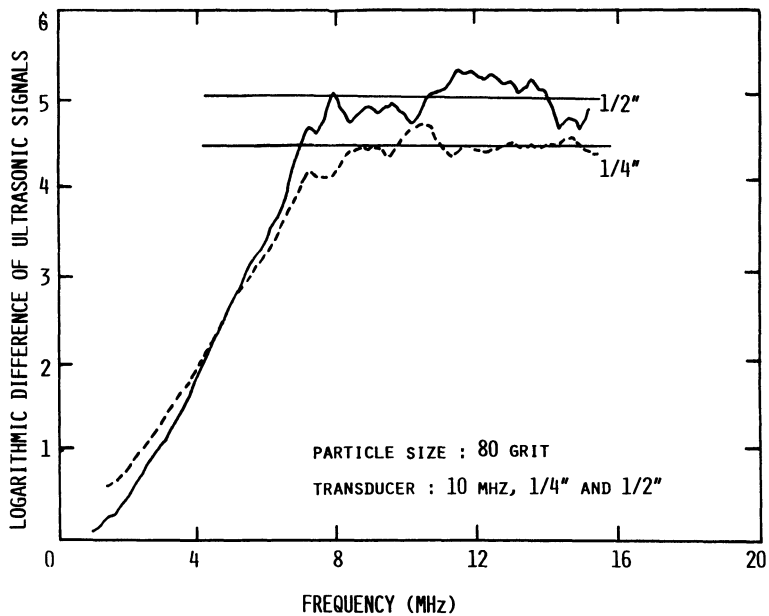


Fig. 6. Shows the signal $S(f)$ for 80 grit sample at two different transducer radii.

ACKNOWLEDGEMENT

This work was sponsored by the Center for Advanced Nondestructive Evaluation, operated by the Ames Laboratory, USDOE, for the Air Force Wright Aeronautical Laboratories/Materials Laboratory under Contract No. W-7405-ENG-82 with Iowa State University.

REFERENCES

1. M. Gzalet, J. Frohly, J. Perdigao and C. Bruneel, *J. Acoust. Soc. Am.*, **76**, 1259 (1984).
2. P. Reinholdsten and B. T. Khuri-Yakub, Review of Progress in Quantitative NDE, **5A**, D. O. Thompson and D. E. Chimenti, Eds., (Plenum Press, NY, 1986), p. 485.
3. E. R. Generazio, Review of Progress in Quantitative NDE, **4A**, D. O. Thompson and D. E. Chimenti, Eds., (Plenum Press, NY, 1985), p. 975.
4. L. Adler, K. Lewis, M. de Billy and G. Quentin, in New Procedures in Nondestructive Testing, Ed., P. Holler, (Pub. Springer-Verlag, Berlin, 1983), p. 163.